

Diagnosis of Early Mild Cognitive Impairment Based on Associated High-Order Functional Connection Network Generated by Multimodal MRI

Weiping Wang¹, Shunqi Zhang, Zhen Wang², Xiong Luo³, Ping Luan, Alexander Hramov, Jürgen Kurths⁴, Chang He, and Jianwu Li

Abstract—Mild cognitive impairment (MCI) is highly likely to convert to Alzheimer’s disease (AD). The main approach to identifying MCI is using a functional connection network (FCN). Traditional FCN is used to study the correlation between two brain regions, but it lacks deeper brain interaction information. Neuroscientists found the internal functional activity pattern in the human brain is characterized by sparse, modular, and overlapping structures, and the FCN is restricted by the brain structural connection network (SCN). They can improve the estimation accuracy of FCN. Therefore, this article first constructs low order FCN (LFCN) based on brain sparse, modular, and overlapping activity patterns. Then, new high-order FCN (HFCN) is proposed based on the restrictive relationship between SCN and FCN. To combine high robustness of LFCN with high sensitivity of HFCN, a new combination strategy of LFCN and HFCN is proposed. It integrates the idea of brain modular and overlapping with the restricted relationship between SCN and FCN. Finally, the experimental results show that in early MCI (EMCI) recognition the best classification performance is acquired with an accuracy of 91.42%, which is better than similar methods. This method will be instrumental in the early recognition of clinical MCI.

Index Terms—Associated high-order functional connectivity network, early diagnosis, mild cognitive impairment (MCI), multimodal magnetic resonance imaging (MRI).

Manuscript received 29 November 2022; revised 16 April 2023; accepted 27 May 2023. Date of publication 14 June 2023; date of current version 9 April 2024. This work was supported in part by the Ministry of Industry and Information Technology Special Fund for High-Quality Development under Grant TC220A04A-182; in part by the Innovation and Transformation Foundation of Peking University Third Hospital under Grant BYSYZHKC2021107; in part by the National Natural Science Foundation of China under Grant 62271045; in part by the National Science Fund for Distinguished Young Scholarship of China under Grant 62025602; in part by the Fundamental Research Funds for the Central Universities under Grant QNXM20220038; in part by the Science and Technology Innovation Special Foundation of Foshan Municipal People’s Government under Grant BK21BF001; in part by the Key Project of Basic Research of Shenzhen under Grant JCYJ20200109113603854; in part by the Key Technology Research and Development Program of Science and Technology Scientific and Technological Innovation Team of Shaanxi Province under Grant 2020TD-013; in part by the Key Program for International Science and Technology Cooperation Projects of China under Grant 2022YFE0112300; and in part by XPLOER PRIZ. (Corresponding authors: Weiping Wang; Zhen Wang.)

Please see the Acknowledgment section of this article for the author affiliations.

Digital Object Identifier 10.1109/TCDS.2023.3283406

I. INTRODUCTION

ALZHEIMER’S disease (AD) is an irreversible degenerative brain disease accompanied by memory, cognitive, and motor disorders [1]. It is most likely the cause that results in dementia. China accounts for about a quarter of the world’s total number of AD patients. Currently, the prevalence rate of AD in China is about 5.6%. By 2050, the number of AD patients in China is expected to exceed 30 million [2], [3]. Early mild cognitive impairment (EMCI) appears between cognitive deterioration that links to age and AD or various kinds of dementia [4]. According to the results of multiple examined studies, 38% of respondents with mild cognitive impairment (MCI) who were tracked for five years or longer suffered from dementia [5]. At present, there is no accurate diagnosis and effective treatment for AD. Researchers generally agree that if patients can be diagnosed when they are in the MCI stage, they may be able to take effective measures to prevent further disease progression [6]. Therefore, the accurate diagnosis of EMCI has an essential impact on early intervention and treatment of preclinical AD.

Since neuroimaging can measure variation in brain function and structure related to diseases of the brain in a noninvasive way, it is extensively applied in the study of brain diseases in recent years, including AD/MCI [7], schizophrenia [8], etc. Structural magnetic resonance imaging (MRI), diffusion tensor imaging (DTI), positron emission tomography (PET), and functional MRI (fMRI) can reveal the structural characteristics and functional activity of the human brain disease in the early stage [9], [10], [11]. Resting state fMRI (rs-fMRI) uses blood oxygenation level dependency (BOLD) signals as neuro electrophysiological indicators, which can catch some spontaneous neural activities in the brain. And, it has been applied in the diagnosis of AD and shown good results [12]. A good mapping mechanism can accurately identify the location of lesions through brain imaging, Yu et al. [13] proposed a multidirectional mapping mechanism, which can effectively capture the significant features of MRI and delineate the subtle lesions. In addition, brain networks based on brain images can also be mapped to the brain. Functional connection network (FCN) on the BOLD signal was applied in the analysis of psychiatric

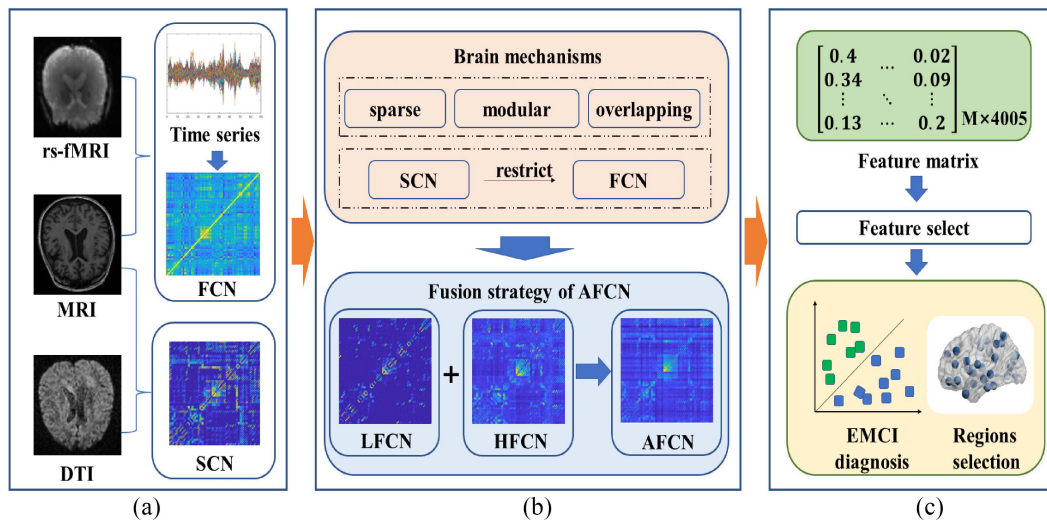


Fig. 1. Flowchart of the proposed framework. (a) Shows the using multimodal data, including MRI, rs-fMRI, and DTI. SCN and BOLD time series are obtained after data processing. (b) Shows the framework structure diagram according to the proposed AFCN method. (c) Shows the process of feature construction and feature selection of AFCN, classification, and regions selection.

disorders [14]. For example, Jitsuishi and Yamaguchi [15] proposed a method to merge FCNs, and it can automatically learn the connections of brain regions. This method was applied to the identification of mental diseases, such as AD and achieved good results. Zhang et al. [16] proposed a modularized framework, which can apply modularized details to discover explicable features from FCN. Nowadays, most FCNs only have the linkage between two brain regions or voxel pairs, and the constructed FCN is also called low order FCN (LFCN). LFCN has the advantage of high robustness to noise, but it is not sensitive to subtle signal changes. Between the EMCI group and the normal control (NC) group, brain network differences are small, so this task is difficult to be completed by the original LFCN. However, improving the accuracy of the FCN could alleviate this problem to some extent.

In recent neuroimaging studies, knowledge of brain mechanisms has been gradually explored. If these brain mechanisms are taken as prior information to estimate FCN, they may act as a pivotal part in the diagnosis of brain diseases. Neuroscientists generally believe that the internal functional activity pattern in the brain is characterized by sparse, modular, and overlapping structures [17], [18], [19]. Lei et al. [20] proposed a feature selection method combining group LASSO and corentropy to reduce dimensions and screen the features of brain regions related to AD, which gained a satisfactory performance in predicting clinical scores of AD. Zhu et al. [21] proposed a synthesis of sparse overlapping modularized (SOM) method to build FCN. They applied it to the identification of depression and got good results. Park and Friston [22] proposed that signal transmission of brain functional networks is limited by large-scale anatomical structure, that is, structural connection network (SCN) has a restrictive relationship to FCN. And Honey et al. [23] proved this theory by a dynamic model. Researchers found that brain regions in the real brain tend to work together, meaning that one brain region can be

influenced by other brain regions. However, LFCN does not reflect this characteristic, and losing high-order knowledge may be important for diagnosing brain diseases. Based on this idea, Jie et al. [24] proposed a method of constructing a functional hyper network, and it indicated that one fringe can integrate with over two brain regions. They applied it to MCI classification and obtained better performance than traditional LFCN methods. And, this brain network is also called high-order FCN (HFCN). However, there is still a long way to go in the construction of HFCN, such as the introduction of the restrictive relationship between SCN and FCN. And it is necessary to propose an effective construction method for HFCN. Therefore, we improve the original HFCN method based on the restriction relation of SCN to FCN.

However, though HFCN can detect subtle changes between brain networks, it lacks the robustness which is important for the diagnosis of EMCI/NC. Hence, some researchers constructed an associated high-order function connection network (AFCN) through the integration of the high robustness of LFCN and the sensitivity of HFCN to different signals. Zhang et al. [25] proposed an AFCN through the combination of LFCN and HFCN. Then, they used the support vector machine (SVM) to classify EMCI and NC and attained fine performance. Zhu et al. [8] put forward an AFCN building strategy that mixed first-order and second-order brain networks and carried out a weighted hybrid of them. However, these methods ignored the advantages of the internal activity pattern in the brain and the restrictive relationship between SCN and FCN.

To address these issues mentioned, this article proposes a new AFCN learning framework. It integrates the sparse, modular, and overlapping activity pattern in the brain and the restrictive relationship between SCN and FCN. We apply it to diagnose EMCI/NC and illustrate the proposed framework in Fig. 1. The following are our main contributions.

TABLE I
DEMOGRAPHIC AND CLINICAL CHARACTERISTICS
OF EMCI PATIENTS AND NC SUBJECTS

Variable	EMCI	NC
Number	52	57
male/female	22/30	32/25
Age(Mean±SD)	75.7±6.8	72.2±6.9

- 1) We build a more accurate LFCN by inherent brain functional activity mode. Then, a new HFCN is constructed based on LFCN and the restricted relationship of SCN to FCN.
- 2) We propose a new fusion strategy that integrates the advantages of brain modular and overlapping with the restricted relationship of SCN on FCN according to the characteristics of LFCN and HFCN.
- 3) This method is applied to the EMCI/NC classification task and the proposed work achieves better performance than typical methods.

II. MATERIALS AND METHODS

A. Data Collection

Three modalities of brain imaging data in the ADNI [26] data set (<https://adni.loni.usc.edu>) are conjointly analyzed in this work, including MRI, rs-fMRI, and DTI. ADNI enables researchers around the world to share data about the early stage of AD. The goal of ADNI is to study MCI and AD intervention, prevention, and treatment by using different biomarkers. We select 109 subjects that have all three modalities, including 52 patients with EMCI (average age 75.8 years, 22 male, and 30 female) and 57 age-matched NC (average age 72.2 years, 32 male, and 25 female). The details of demographics and clinical characteristics are described in Table I.

B. Data Description and Preprocessing

1) *Data Description*: The MRI data has field strength = 3.0 Tesla, FA = 90.0°, matrix = 240.0 × 256.0 × 176.0, slice thickness = 1.0 mm, pixel spacing = 1.0 × 1.0 mm and TR = 2300 ms. The DTI data has strength = 3.0 Tesla, FA = 90.0°, gradient directions = 54.0, matrix = 1044.0 × 1044.0 × 55.0, pixel spacing = 1.0 × 1.0 mm, slice thickness = 2.0 mm, and TR/TE = 7200/56 ms. The rs-fMRI data has field strength = 3.0 Tesla, slice thickness = 3.4 mm, FA = 90.0°, matrix = 448 × 448, pixel spacing = 3.4 × 3.4 mm and TR/TE = 3000.0/30.0 ms. Subjects are required to keep their eyes open and remain relaxed and awake during the scan.

2) *Data Preprocessing*: The rs-fMRI images are preprocessed through DPARSF [27] toolbox (<http://rfmri.org/DPARSF>). We convert these images to neuroimaging informatics technology initiative (NIfTI) file format. To eliminate the effect of noise generated by the subject's adaptation process during the initial scan, for each subject, we delete the first ten time points. We conduct the steps, including slice timing correction, register between rs-fMRI and MRI, motion rectification, normalization, smoothing, and bandpass filtering. Then, we follow the

automatic labeling (AAL) template [28] for registration into rs-fMRI images and segment the brain space into 90 ROIs. Finally, the time series of each subject is acquired from the BOLD signals of all voxels. For the structural images, we use the PANDA toolbox (<http://www.nitrc.org/projects/panda>) and FreeSurfer V6.00 (<https://surfer.nmr.mgh.harvard.edu>) to perform image preprocessing steps. First, skull removal is performed on the MRI images. Then, in order to eliminate the noise during scanning, the head motion correction operation is carried out. In order to avoid the influence of different subjects' brain sizes, spatial standardization operation is carried out. Finally, the AAL template is applied to segment the brain space into 90 ROIs. MRI images are mainly used as templates for the construction of DTI. For DTI images, format conversion and skull removal are performed first. In order to alleviate the vortex distortion image, we use eddy current correction to make the imaging results more accurate. We calibrate head motion, calculated fractional anisotropy (FA) for each voxel, and register it with pretreated MRI. We gain 90 ROIs based on the AAL template partition and then build the SCN based on the FA.

C. Construction of LFCN Based on SOM

Assuming the number of subjects is M , the BOLD signal of the m th subject is described as $X^m \in \mathbb{R}_{N \times t} (m = 1, \dots, M)$ where N and t , respectively, represent the number of brain regions and the length of time signals series.

After obtaining the BOLD time series of the subjects, low-order FCN can be obtained by FCN estimation methods (such as Pearson correlation coefficient (PC), inverse covariance matrix, etc.). However, due to the impact of noise during data collection and processing, the obtained FCNs at this time often have many redundancy and wrong connections, so it is necessary to sparse FCNs. Cognitive scientists agree that not only is brain function modular but that these modules overlap and interact spatially. Therefore, we obtain LFCN based on the SOM method proposed by Zhu et al. [21].

The number of brain modules is set as K in advance, and then FCN is divided into K viable modules through optimization iteration. SOM can estimate LFCN through data-driven methods. We use $\hat{\Theta}$ to represent the LFCN estimated by SOM. The objective function is as follows:

$$\begin{aligned} \hat{\Theta}^m = \arg \min_{\Theta^m, Z^m} & \|X^m - X^m \Theta^m\|_F^2 + \lambda_1 \|\Theta^m\|_* \\ & + \lambda_2 \left(\|\Theta^m\|_1 - \text{tr}(Z^m (Z^m)^T | \Theta^m) \right) \\ \text{s.t.} & \|Z^m\|_2 \leq \sqrt{N/2K}, \|Z_i^m\|_2 \leq 1, \|Z^m\|_F \leq \sqrt{N/2}. \end{aligned} \quad (1)$$

It could be also written as

$$\begin{aligned} \hat{\Theta}^m = \arg \min_{\Theta^m, Z^m} & \|X^m - X^m \Theta^m\|_F^2 + \lambda_1 \|\Theta^m\|_* \\ & + \sum_{i,j} \lambda_2 \left(1 - (Z^m (Z^m)^T)_{ij} \right) |\theta_{ij}^m| \\ \text{s.t.} & \|Z^m\|_2 \leq \sqrt{N/2K}, \|Z_i^m\|_2 \leq 1, \|Z^m\|_F \leq \sqrt{N/2} \end{aligned} \quad (2)$$

where m represents the m th subject, λ_1 and λ_2 are non-negative tuning parameters. As the number of modules, K is a default

value. $Z \in N \times K$ represents the emergence of overlapping mechanism because it represents the allocation information of variables in each K module, and each ROI can be distributed to different modules. Z_i stands for the i th row of Z , which means the probability of a certain ROI belongs to each module.

D. Construction of HFCN

Since HFCN can take into account the influence of other brain regions on a certain brain region that is more sensitive to slight differences, so we construct HFCN based on the obtained LFCN. According to the restrictive relationship between brain SCN and brain FCN, we further calculate LFCN using the following formula:

$$L_{ij}^m = \begin{cases} 0, & \text{if } SC_{ij}^m = 0 \\ \hat{\Theta}_{ij}^m, & \text{otherwise} \end{cases} \quad (3)$$

where m represents the m th subject, i and j represent the indexes of ROI, respectively. $\hat{\Theta}_{ij}^m$ and SC_{ij}^m , respectively, represent the LFCN strength and SCN strength between the i th ROI and j th ROI of the m th subject.

Research indicated that the brain network method through PC can represent the interaction between brain regions or neurons [29]. After obtaining LFCN, we construct HFCN based on the Pearson PC. The calculation method is as follows:

$$H_{ij}^m = \frac{(L_i^m - \bar{L}_i^m)^T (L_j^m - \bar{L}_j^m)}{\sqrt{(L_i^m - \bar{L}_i^m)^T (L_i^m - \bar{L}_i^m)} \sqrt{(L_j^m - \bar{L}_j^m)^T (L_j^m - \bar{L}_j^m)}} \quad (4)$$

where $H \in N \times N$ means the matrix of HFCN, L_i^m is the i th row of LFCN of the m th subject, \bar{L}_i^m means value vector of L_i^m . A HFCN is constructed which retains second-order information between brain regions. And, it is more sensitive to changes in brain networks, which can capture more information.

E. Construction of AFCN With LFCN and HFCN

LFCN and HFCN construct brain connectivity at different levels and angles. The former is more robust to noise transmission, while the latter is more sensitive to subtle signal differences. There are complementary features in the two approaches for diagnostic tasks. Inspired by the above problems, the HFCNs and LFCNs are associated to construct AFCNs. The details are as follows:

$$A^m = \lambda(U^m \circ L^m) + (1 - \lambda)V^m H^m \quad (5)$$

where $\lambda \in [0, 1]$ is weight parameter, L^m is the LFCN of the m th subject and H^m is the HFCN of the m th subject. \circ means Hadamard product, $U^m, V^m \in 90 \times 90$ are coefficient matrixes. U^m is the mapping matrix of the m th subject's SCN, and the calculation of V^m is as follows:

$$V_{ij}^m = \begin{cases} 0, & \text{if } SC_{ij}^m = 0 \\ k, & \text{otherwise} \end{cases} \quad (6)$$

where k is the number of common modules where the i th ROI and the j th ROI are located.

In AFCN, LFCN retains the original connection strength between two brain regions, while HFCN captures the connection strength of a certain brain region and its adjacent brain regions. The proposed AFCN characterizes the high-level functional interactions between HFCN and LFCN networks and fuses their complementary relationships to explore new relationships between brain regions. Therefore, the proposed hybrid model can balance the robustness and classification performance.

F. Feature Extraction/Selection

Once we have obtained effective FCNs for all subjects, the next task becomes extracting features from the estimated FCN for the recognition of subjects from NC and EMCI. How select effective features turn out to be the problem. Disease identification based on FCN usually adopts two strategies. One is to extract features by some graph measures, such as clustering coefficient and node degree [30]; the other is to use network connection weights as features [15]. Since different graph metrics capture different aspects of network attributes, extracting different graph theoretic attributes as features may affect the classification results of FCN. Therefore, in our experiment, we use the connection weights of FCN as features to eliminate the effect of different features on the verification of FCN itself. The use of network connection weights as features theoretically contains all the network information, but it leads to high dimensional problems.

For instance, an undirected network graph with N nodes has $N(N-1)/2$ edges. In this work, $N = 90$, so the characteristic dimension is 4005. To remove redundant features from high-dimensional data, in this article, we apply maximum correlation and minimum redundancy (mRMR) methods [31] to analyze the importance of different features. Each feature can be sorted according to its correlation with the target variable, and the redundancy of these features would be considered in the sorting process. A good feature is defined as one that has the best tradeoff between minimum redundancy and maximum correlation.

G. Experimental Setting

We adopt the tenfold cross-validation strategy in our experiments. Specially, all subjects are divided into ten equal portions. We choose one part in turn as the test set and the rest for training. We evaluate the performance using SVM with Gaussian kernel for each specific test. To reduce the error, we repeated the whole process 100 times. We use accuracy (ACC), positive predict value (PPV), sensitivity (SEN), specificity (SPE), class balanced accuracy (BAC), F1 score (F1), and the area under the receiver operating characteristic curve (AUC) to measure diagnosis performance. The details are as follows:

$$ACC = \frac{TP + TN}{TP + TN + FN + FP} \quad (7)$$

$$PPV = \frac{TP}{TP + FP} \quad (8)$$

$$SEN = \frac{TP}{TP + FN} \quad (9)$$

$$\text{SPE} = \frac{\text{TN}}{\text{TN} + \text{FP}} \quad (10)$$

$$\text{BAC} = \frac{\text{SEN} + \text{SPE}}{2} \quad (11)$$

$$\text{F1} = \frac{2 \cdot \text{PPV} \cdot \text{SEN}}{\text{PPV} + \text{SEN}} \quad (12)$$

where TP means true positive, TN means true negative, FP means false positive, and FN means false negative, respectively. AUC is defined as the area under the ROC curve and the coordinate axis.

H. Comparison Methods

The following FCN construction methods and sparse approaches are chosen as comparison methods: LFCN (Th_LFCN) and HFCN (Th_HFCN) constructed based on the threshold method [32], LFCN (MST_LFCN) and HFCN (MST_HFCN) constructed based on minimum spanning tree [33]; LFCN (SOM_LFCN) and HFCN(SOM_HFCN) constructed based on SOM method; the hybrid high-order brain network (AFCN1) proposed by [8]; the hybrid high-order brain network (AFCN2) proposed by [25]. In addition, logistic regression (LR) and K nearest neighbor (KNN) [34], [35] are also used for auxiliary comparative experimentations to ascertain the usefulness of our proposed strategy.

III. RESULTS

A. Influence of Feature Number on Classification Results

If complex classification features are applied to a limited training sample, it tends to overfit the data. Apart from overfitting, it is tough to determine appropriate hyperparameters involved in classification models without sufficient training samples. In order to identify valid brain network regions and connections, the selection of the number of features used for classification tasks is important. As for the number of features, we first conduct a comparative experiment with a step size of 20 within the range of [10, 1000], as shown in Fig. 2(a) and (b). We can obtain that the best number of features is within the range of [10, 200] from the experimental outcomes. Therefore, a comparative experiment with a step size of 2 is conducted within the range of [10, 200], with a total of 95 candidate values. From Fig. 2(c) and (d), the classification performance is the best when the number of features is 92.

B. Influence of λ on Classification Results in AFCN

To explore the influence of λ on classification results and determine the best value of λ , we conduct λ set of experiments with a step size of 0.02 within the range of [0,1]. We can see the results in Fig. 3.

From Fig. 3, we get the best performance when λ is 0.28. In other words, in the best AFCN constructed, the latter, HFCN, accounts for a higher proportion, which means that HFCN may be more important than LFCN. We suspect that HFCN may be more sensitive to subtle differences in different types of signals, and that can better identify EMCI and NC.

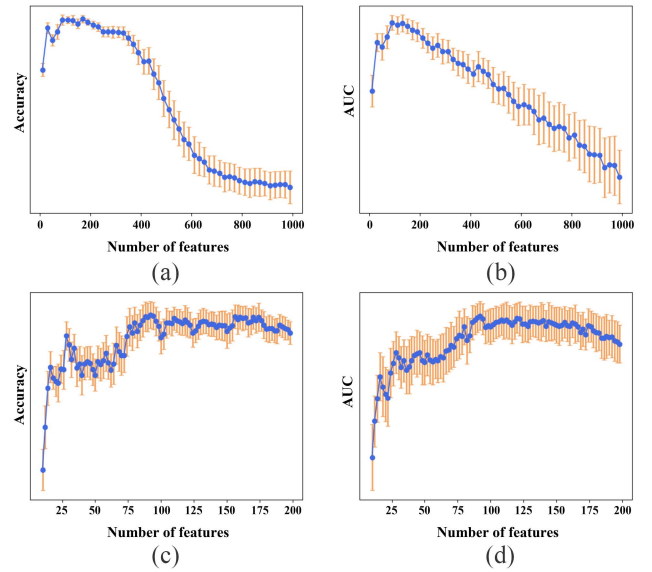


Fig. 2. Influence of different numbers of features on classification results. The x -axis describes the number of features, and the y -axis means the size of relevant evaluation indicators. Each value experiment is repeated 100 times, with the blue dot representing the mean of 100 experiments and the orange line representing the standard deviation. (a) Accuracy when the number of feature range is set to [10, 1000]. (b) AUC when the number of feature range is set to [10, 1000]. (c) Accuracy when the number of feature range is set to [10, 200]. (d) AUC when the number of feature range is set to [10, 200].

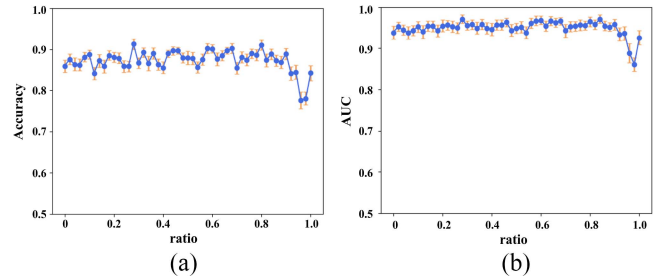


Fig. 3. Influence of λ on classification results. (a) Accuracy varies with λ . (b) AUC varies with λ .

C. Classification Results Using Different Methods

In order to construct brain networks by different methods, we use SVM as the classifier to do a series of comparative experiments, the details of experimental settings are described in Section II-G. The results can be found in Table II and Fig. 4. We can obtain that our strategy gets the best performance over other methods. Specifically, the classification accuracy and balance accuracy of this method is 91.42% and 91.33%, while the best accuracy and balance accuracy of other methods are only 88.81% and 89.63%. The comprehensive performance indexes reveal that the AUC is 0.972 and the F1 score is 0.912, which proves that our proposed method has excellent diagnostic ability.

In order to prove the validity of the method from other perspectives, LR and KNN are introduced as classifiers to carry out a set of comparative experiments. The specific experimental performance can be displayed in Table III.

TABLE II
PERFORMANCE OF DIFFERENT METHODS IN CLASSIFICATION OF NC/EMCI

Method	ACC	PPV	SEN	SPE	BAC	AUC	F1
Th_LFCN	80.24±1.67	82.06±2.23	80.48±3.37	80.30±2.36	80.39±4.30	87.89±1.78	79.74±2.33
Th_HFCN	81.03±2.51	88.78±2.36	73.21±3.24	89.96±3.16	81.58±5.46	90.32±1.96	78.52±3.31
MST_LFCN	84.81±1.85	81.53±2.28	91.60±2.86	77.26±3.36	84.43±4.21	93.27±1.38	85.46±2.21
MST_HFCN	85.52±1.65	86.54±2.37	86.72±2.60	85.25±2.86	85.98±3.92	93.57±1.80	85.14±2.17
SOM_LFCN	84.61±1.32	85.25±1.78	86.30±2.40	83.05±2.37	84.67±3.36	95.58±1.37	84.56±1.70
SOM_HFCN	88.75±1.78	89.26±2.32	91.12±2.45	88.09±3.03	89.60±3.95	96.77±0.96	89.02±2.25
AFCN1	88.81±1.36	88.14±2.25	91.23±1.99	88.04±3.15	89.63±3.21	95.40±1.59	88.92±1.75
AFCN2	83.59±1.93	87.89±2.86	80.27±2.92	87.99±3.09	84.13±4.57	94.99±1.54	82.48±2.50
SOM_AFCN(proposed)	91.42±1.19	90.05±2.22	94.14±1.33	88.52±2.77	91.33±2.50	97.20±1.02	91.20±1.53

TABLE III
PERFORMANCE OF DIFFERENT CLASSIFIERS IN LFCN, HFCN, AND AFCN

Method	ACC	PPV	SEN	SPE	BAC	AUC	F1
LR_LFCN	84.45±1.26	87.09±2.03	85.95±2.35	83.18±2.35	84.56±3.87	95.74±1.24	83.92±2.31
KNN_LFCN	84.96±1.24	85.15±1.95	86.88±2.37	83.06±2.43	84.97±3.41	95.65±1.34	84.75±1.83
SVM_LFCN	84.61±1.32	85.25±1.78	86.30±2.40	83.05±2.37	84.67±3.36	95.58±1.37	84.56±1.70
LR_HFCN	89.01±1.83	89.89±2.35	90.84±2.31	88.82±2.50	89.83±3.54	96.89±1.06	89.31±2.09
KNN_HFCN	88.43±1.97	89.36±2.46	91.37±2.31	87.49±3.16	89.43±3.83	96.80±1.13	88.55±2.16
SVM_HFCN	88.75±1.78	89.26±2.32	91.12±2.45	88.09±3.03	89.60±3.95	96.77±0.96	89.02±2.25
LR_AFCN	91.15±1.35	89.79±2.22	94.18±1.40	87.95±2.58	91.06±2.94	97.01±1.16	91.07±1.78
KNN_AFCN	91.19±1.25	89.67±2.31	94.23±1.42	88.02±2.63	91.12±2.80	97.34±1.24	91.19±1.69
SVM_AFCN	91.42±1.19	90.05±2.22	94.14±1.33	88.52±2.77	91.33±2.50	97.20±1.02	91.20±1.53

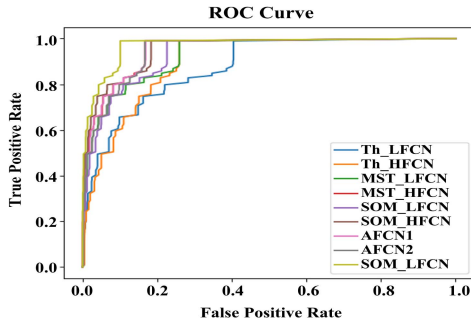


Fig. 4. ROC curves for all methods.

From Table III, all three classifiers perform best when using the AFCN method we proposed. And, HFCN has better performance than LFCN. It also proves that the proposed method has strong robustness.

D. Classification Results Using Different Smoothing Kernels

In this article, we use smooth kernel $\text{FWHM} = 4$ mm for the fMRI data processing. Since smoothing may affect the structure and properties of functional brain networks in a nontrivial way [36], [37]. In particular, smoothing affects the differences in network structure observed between patients and healthy controls [38]. Considering this effect, the SOM_AFCN method proposed in this article is used for the following comparative experiments with a set of smoothed kernel FWHMs. Triana et al. [38] proposed that large smoothing kernels are rarely used in practice, and the main task of this article is to classify EMCI/NC, so small smoothing kernels are mainly selected for the experiment. In this article, $\text{FWHM} = 4$ mm is selected as the baseline of this comparison experiment. And no smoothing, $\text{FWHM} = 6$ mm and $\text{FWHM} = 8$ mm are

selected as comparison methods based on the data format. The experimental performance can be displayed in Table IV.

The experimental results show that for the SOM_AFCN model, using a small smoothing kernel seems to get better results than no smoothing. Moreover, the smooth kernel $\text{FWHM} = 4$ mm performs better than $\text{FWHM} = 6$ mm and $\text{FWHM} = 8$ mm. There is no significant difference between smooth kernel size $\text{FWHM} = 6$ mm and $\text{FWHM} = 8$ mm. Overall, in this article, using a small smoothing kernel ($\text{FWHM} = 4$ mm) has the best results for EMCI/NC classification. Therefore, the results prove that the AFCN method in this article is effective.

IV. DISCUSSION

In this article, a new AFCN construction framework is put forward, which integrates sparse, modular, and overlapping activity patterns and the restricted relationship between SCN and FCN. Specifically, we first build a more accurate LFCN by SOM model. Then, a new HFCN is constructed by the restricted relationship of SCN to FCN. LFCN has good robustness and high tolerance to external noise. HFCN can reflect the impact of other ROIs on a certain ROI, which is more consistent with real brain mechanisms. And, HFCN is more sensitive to subtle differences in signals. Based on the above factors, we design a new AFCN framework to fuse LFCN and HFCN. In the EMCI/NC classification task, we have proved the feasibility and superiority of our strategy. The average LFCN, HFCN and AFCN of NC group and EMCI group are visualized in Fig. 5, and we also plot the differences between them based on the NC group. From Fig. 5(g)–(i), the difference between NC and EMCI in the brain FCN constructed by the LFCN method is smaller than that in the other two groups. And there are more

TABLE IV
CLASSIFICATION PERFORMANCE OF DIFFERENT SMOOTHING KERNELS USING SOM_AFCN

Smoothing	ACC	PPV	SEN	SPE	BAC	AUC	F1
No	88.18±1.28	89.03±1.65	88.58±2.43	88.25±2.20	88.42±2.67	95.25±1.48	87.86±1.65
[4, 4, 4]	91.42±1.19	90.05±2.22	94.14±1.33	88.52±2.77	91.33±2.50	97.20±1.02	91.20±1.53
[6, 6, 6]	90.25±1.34	89.79±2.08	92.44±1.91	88.19±2.58	90.31±2.61	96.1±1.12	90.33±1.51
[8, 8, 8]	90.57±1.21	91.20±2.15	90.90±2.16	90.29±1.97	90.59±2.72	96.0±1.06	90.30±1.64

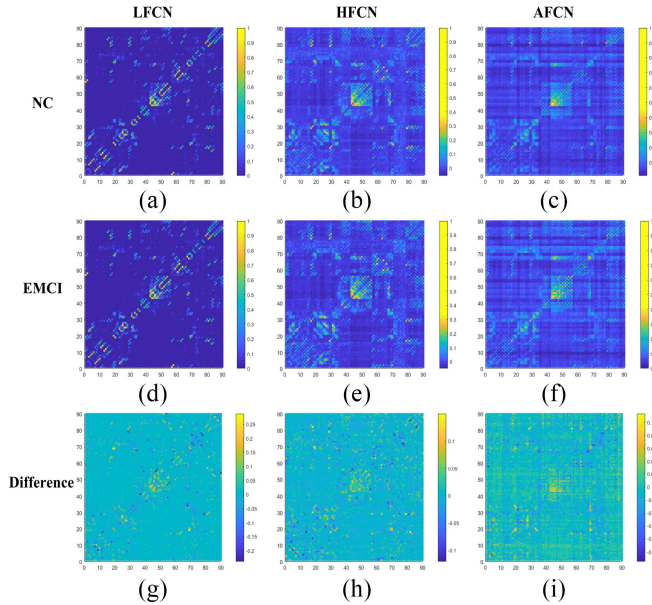


Fig. 5. Average LFCN, HFCN and AFCN of NC group and EMCI group, as well as the differences of different methods based on NC. The x -axis and y -axis represent the indexes of ROIs. (a)–(c) Mean LFCN, HFCN, and AFCN of the NC group. (d)–(f) Mean LFCN, HFCN, and AFCN of the EMCI group. (g) Difference between the mean LFCN, HFCN and AFCN of the NC group and that of the EMCI group.

differences in AFCN, which also proves the superiority of our method.

According to the feature selection in the experiment of NC and EMCI, we select the top 25 important connections of ROI, and the details are shown in Table V. In order to know more clearly how these connections are connected in the brain, we make a visualization of these connections in Fig. 6.

As is depicted in Table V and Fig. 6, the connections between the Inferior gyrus, opercular part, and other brain regions are significantly altered, and [39] could support our findings. The connection between Superior occipital gyrus and other brain regions, Middle frontal gyrus, and Precentral gyrus also change significantly, and similar findings could be found in some studies [40], [41]. From Table V and Fig. 6, some brain regions show up multiple times, which suggests that they may act as an essential part of analyzing differences between the EMCI and NC groups.

Then, we count the repeated brain regions, sort them according to the order and frequency of their occurrence, and then standardize the weights. The ten most momentous ROIs are exhibited in Table VI and Fig. 7.

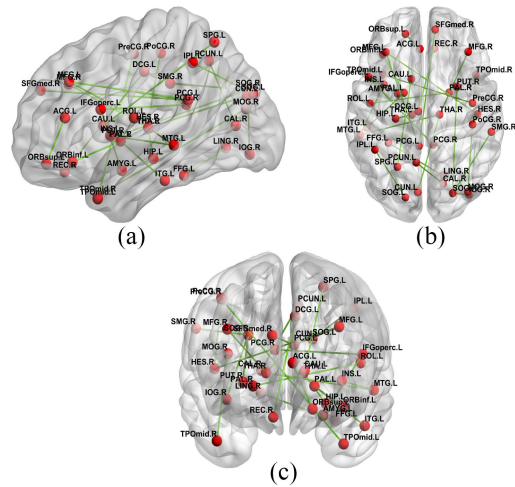


Fig. 6. Top 25 important brain network connections are displayed in different view directions. (a) View direction: sagittal. (b) View direction: axial. (c) View direction: corona.

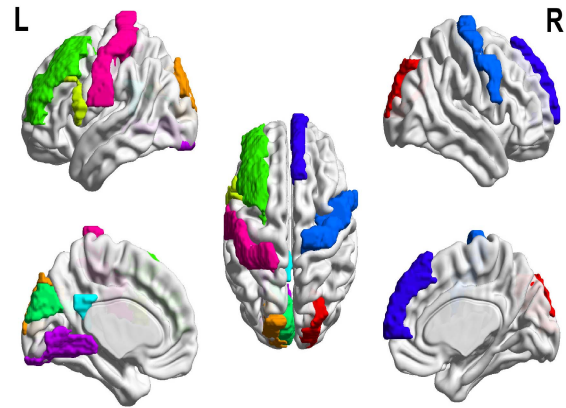


Fig. 7. Top 10 significant alterations of brain ROIs selected by features.

As shown in Table VI and Fig. 7, we select the areas of Superior occipital gyrus, L.Inferior frontal gyrus, opercular part, L.Middle frontal gyrus, L.Cuneus, L.Lingual gyrus, etc., which means that these ROIs may be the key regions for differences between EMCI and NC. Superior occipital gyrus is mainly responsible for object recognition, including the functional characteristics of objects [42]. Inferior frontal gyrus, opercular part is associated with recognizing a tone of voice in spoken native languages [43]. The medial frontal gyrus is associated with literacy and numeracy [44]. The Cuneus is associated with visual signal processing [45]. The Posterior cingulate gyrus has been found to be associated with spatial memory and configural learning [46], and the lingual gyrus is associated with image analysis and visual memory

TABLE V
TOP 25 IMPORTANT BRAIN NETWORK CONNECTIONS BETWEEN EMCI GROUP AND NC GROUP

No.	Brain region A		Brain region B	
1	IFGoperc.L	L.Inferior frontal gyrus, opercular part	AMYG.L	L.Amygdala
2	SOG.R	R.Superior occipital gyrus	SMG.R	R.Supramarginal gyrus
3	MFG.R	R.Middle frontal gyrus	THA.R	R.Thalamus
4	SOG.R	R.Superior occipital gyrus	IOG.R	R.Inferior occipital gyrus
5	HIPL	L.Hippocampus	THA.L	L.Thalamus
6	IFGoperc.L	L.Inferior frontal gyrus, opercular part	PCG.R	R.Posterior cingulate gyrus
7	PoCG.R	R.Postcentral gyrus	HES.R	R.Heschl gyrus
8	MFG.L	L.Middle frontal gyrus	HES.R	R.Heschl gyrus
9	THA.R	R.Thalamus	MTG.L	L.Middle temporal gyrus
10	ORBinf.L	L.Inferior frontal gyrus, orbital part	PAL.L	L.Lenticular nucleus, pallidum
11	LING.R	R.Lingual gyrus	FFG.L	L.Fusiform gyrus
12	MFG.L	L.Middle frontal gyrus	PCG.L	L.Posterior cingulate gyrus
13	PAL.L	L.Lenticular nucleus, pallidum	ITG.L	L.Inferior temporal gyrus
14	SPG.L	L.Superior parietal gyrus	CAU.L	L.Caudate nucleus
15	SOG.R	R.Superior occipital gyrus	PUT.R	R.Lenticular nucleus, putamen
16	ORBsup.L	L.Superior frontal gyrus, orbital part	ACG.L	L.Anterior cingulate and paracingulate gyri
17	MOG.R	R.Middle occipital gyrus	TPOmid.R	R.Temporal pole: middle temporal gyrus
18	PreCG.R	R.Precentral gyrus	TPOmid.L	L.Temporal pole: middle temporal gyrus
19	SOG.L	L.Superior occipital gyrus	IPL.L	L.Inferior parietal, but supramarginal and angular gyri
20	ROL.L	L.Rolandic operculum	PAL.R	R.Lenticular nucleus, pallidum
21	REC.R	R.Gyrus rectus	DCG.L	L.Median cingulate and paracingulate gyri
22	CUN.L	L.Cuneus	THA.R	R.Thalamus
23	SFGmed.R	R.Superior frontal gyrus, medial	PCG.L	L.Posterior cingulate gyrus
24	CAL.R	R.Calcarine fissure and surrounding cortex	PCUN.L	L.Precuneus
25	INS.L	L.Insula	MTG.L	L.Middle temporal gyrus

TABLE VI
TOP 10 SIGNIFICANT ROIS BETWEEN EMCI GROUP AND NC GROUP

No.	Brain ROI	Weight
1	R.Superior occipital gyrus	1.000
2	L.Superior occipital gyrus	0.7705
3	L.Inferior frontal gyrus, opercular part	0.6856
4	L.Middle frontal gyrus	0.6742
5	L.Cuneus	0.6119
6	L.Posterior cingulate gyrus	0.4929
7	R.Precentral gyrus	0.4816
8	R.Superior frontal gyrus, medial	0.4703
9	L.Lingual gyrus	0.4476
10	L.Postcentral gyrus	0.4136

storage [42], [43], [44], [45]. These ROIs may become beneficial for MCI-related diagnoses, which could be discovered in previous studies [47], [48], [49], [50].

V. CONCLUSION

In summary, according to the characteristics of LFCN and HFCN, we propose a new combination strategy of LFCN and HFCN, which integrates the idea of brain modular and overlapping with the restricted relationship between SCN and FCN. The method also combines the high robustness of LFCN with the high sensitivity of HFCN. It provides fresh thought for brain disease classification tasks by brain networks. We apply it to the diagnosis of EMCI/NC and get good performance. Besides, the robustness of the proposed method is verified in experiments. Our work also shows that brain mechanisms play a great role in the construction of brain networks. However, insufficient data is still a major defect of this experiment. Hence, we will expand the data set from many aspects to enhance the model's robustness in the future. What is more, with the development of brain science, the accuracy of brain

network model will be closer to that of human brain. Deep learning as an important tool has achieved great success in image, text, and other fields. The combination with deep learning is expected to further improve the precision and scale of brain network construction, and there may be a lot of meaningful exploration work in the field of brain science.

ACKNOWLEDGMENT

Weiping Wang and Xiong Luo are with the School of Computer and Communication Engineering and the Beijing Key Laboratory of Knowledge Engineering for Materials Science, University of Science and Technology Beijing, Beijing 100083, China, also with the Shunde Graduate School, University of Science and Technology Beijing, Foshan 528399, Guangdong, China (e-mail: weipingwangjt@ustb.edu.cn).

Shunqi Zhang and Chang He are with the School of Computer and Communication Engineering, University of Science and Technology Beijing, Beijing 100083, China.

Zhen Wang is with the School of Cyberspace and the School of Artificial Intelligence, Optics, and Electronics, Northwestern Polytechnical University, Xi'an 710072, China (e-mail: nkzhenwang@163.com).

Ping Luan is with the Guangdong Second Provincial General Hospital and Health Science Center, Shenzhen University, Shenzhen 518060, China.

Alexander Hramov is with the Center for Technologies in Robotics and Mechatronics Components, Innopolis University, 420500 Innopolis, Russia, and also with the Institute of Cardiological Research, Saratov State Medical University, 410012 Saratov, Russia.

Jürgen Kurths is with the Institute of Physics, Humboldt University of Berlin, 10099 Berlin, Germany, and also with the the Research Department Complexity Sciences, Potsdam Institute for Climate Impact Research, 14473 Potsdam, Germany.

Jianwu Li is with the Institute of Frontier Technology, Beijing Institute of Technology, Jinan 250300, China, and also with the Department of Engineering, Huanghe Science and Technology College, Zhengzhou 450000, China.

REFERENCES

- [1] R. S. Wilson, E. Segawa, P. A. Boyle, S. E. Anagnos, L. P. Hizek, and D. A. Bennett, "The natural history of cognitive decline in Alzheimer's disease," *Psychol. Aging*, vol. 27, no. 4, p. 1008, 2012.
- [2] Alzheimer's Association, "2019 Alzheimer's disease facts and figures," *Alzheimer's Dementia*, vol. 15, no. 3, pp. 321–387, 2019.

- [3] L. Jia et al., "Dementia in China: Epidemiology, clinical management, and research advances," *Lancet Neurol.*, vol. 19, no. 1, pp. 81–92, 2020.
- [4] S. Gauthier et al., "Mild cognitive impairment," *Lancet*, vol. 367, no. 9518, pp. 1262–1270, 2006.
- [5] A. J. Mitchell and M. Shiri-Feshki, "Rate of progression of mild cognitive impairment to dementia—meta-analysis of 41 robust inception cohort studies," *Acta Psychiatrica Scandinavica*, vol. 119, no. 4, pp. 252–265, 2009.
- [6] S. Wang, H. Wang, Y. Shen, and X. Wang, "Automatic recognition of mild cognitive impairment and Alzheimers disease using ensemble based 3D densely connected convolutional networks," in *Proc. 17th IEEE Int. Conf. Mach. Learn. Appl. (ICMLA)*, 2018, pp. 517–523.
- [7] W. Yu, B. Lei, M. K. Ng, A. C. Cheung, Y. Shen, and S. Wang, "Tensorizing GAN with high-order pooling for Alzheimer's disease assessment," *IEEE Trans. Neural Netw. Learn. Syst.*, vol. 33, no. 9, pp. 4945–4959, Sep. 2021.
- [8] Q. Zhu, H. Li, J. Huang, X. Xu, D. Guan, and D. Zhang, "Hybrid functional brain network with first-order and second-order information for computer-aided diagnosis of schizophrenia," *Front. Neurosci.*, vol. 13, p. 603, Jun. 2019.
- [9] J. Venugopalan, L. Tong, H. R. Hassanzadeh, and M. D. Wang, "Multimodal deep learning models for early detection of Alzheimer's disease stage," *Sci. Rep.*, vol. 11, no. 1, p. 3254, 2021.
- [10] S. You et al., "Fine perceptive GANs for brain MR image super-resolution in wavelet domain," *IEEE Trans. Neural Netw. Learn. Syst.*, early access, Mar. 7, 2022, doi: [10.1109/TNNLS.2022.3153088](https://doi.org/10.1109/TNNLS.2022.3153088).
- [11] S. Hu, W. Yu, Z. Chen, and S. Wang, "Medical image reconstruction using generative adversarial network for Alzheimer disease assessment with class-imbalance problem," in *Proc. IEEE 6th Int. Conf. Comput. Commun. (ICCC)*, 2020, pp. 1323–1327.
- [12] K. Wang et al., "Altered functional connectivity in early Alzheimer's disease: A resting-state fMRI study," *Human Brain Map.*, vol. 28, no. 10, pp. 967–978, 2007.
- [13] W. Yu et al., "Morphological feature visualization of Alzheimer's disease via multidirectional perception GAN," *IEEE Trans. Neural Netw. Learn. Syst.*, early access, Mar. 23, 2022, doi: [10.1109/TNNLS.2021.3118369](https://doi.org/10.1109/TNNLS.2021.3118369).
- [14] R. F. Betzel and D. S. Bassett, "Multi-scale brain networks," *Neuroimage*, vol. 160, pp. 73–83, Oct. 2017.
- [15] T. Jitsuishi and A. Yamaguchi, "Searching for optimal machine learning model to classify mild cognitive impairment (MCI) subtypes using multimodal MRI data," *Sci. Rep.*, vol. 12, no. 1, pp. 1–14, 2022.
- [16] Y. Zhang, X. Jiang, L. Qiao, and M. Liu, "Modularity-guided functional brain network analysis for early-stage dementia identification," *Front. Neurosci.*, vol. 15, Aug. 2021, Art. no. 720909.
- [17] X. Jiang et al., "Temporal dynamics assessment of spatial overlap pattern of functional brain networks reveals novel functional architecture of cerebral cortex," *IEEE Trans. Biomed. Eng.*, vol. 65, no. 6, pp. 1183–1192, Jun. 2018.
- [18] G. L. Baum et al., "Development of structure–function coupling in human brain networks during youth," *Proc. Nat. Acad. Sci.*, vol. 117, no. 1, pp. 771–778, 2020.
- [19] J. Yuan et al., "Spatio-temporal modeling of connectome-scale brain network interactions via time-evolving graphs," *Neuroimage*, vol. 180, pp. 350–369, Oct. 2018.
- [20] B. Lei et al., "Predicting clinical scores for Alzheimer's disease based on joint and deep learning," *Expert Syst. Appl.*, vol. 187, Jan. 2022, Art. no. 115966.
- [21] Z. Zhu, Z. Zhen, X. Wu, and S. Li, "Estimating functional connectivity by integration of inherent brain function activity pattern priors," *IEEE/ACM Trans. Comput. Biol. Bioinf.*, vol. 18, no. 6, pp. 2420–2430, Nov./Dec. 2021.
- [22] H.-J. Park and K. Friston, "Structural and functional brain networks: From connections to cognition," *Science*, vol. 342, no. 6158, 2013, Art. no. 1238411.
- [23] C. J. Honey et al., "Predicting human resting-state functional connectivity from structural connectivity," *Proc. Nat. Acad. Sci.*, vol. 106, no. 6, pp. 2035–2040, 2009.
- [24] B. Jie, C.-Y. Wee, D. Shen, and D. Zhang, "Hyper-connectivity of functional networks for brain disease diagnosis," *Med. Image Anal.*, vol. 32, pp. 84–100, Aug. 2016.
- [25] Y. Zhang, H. Zhang, X. Chen, S.-W. Lee, and D. Shen, "Hybrid high-order functional connectivity networks using resting-state functional MRI for mild cognitive impairment diagnosis," *Sci. Rep.*, vol. 7, no. 1, pp. 1–15, 2017.
- [26] C. R. Jack Jr. et al., "The Alzheimer's disease neuroimaging initiative (ADNI): MRI methods," *J. Magn. Reson. Imag.*, vol. 27, no. 4, pp. 685–691, 2008.
- [27] C.-G. Yan, X.-D. Wang, X.-N. Zuo, and Y.-F. Zang, "DPABI: Data processing & analysis for (resting-state) brain imaging," *Neuroinformatics*, vol. 14, no. 3, pp. 339–351, 2016.
- [28] N. Tzourio-Mazoyer et al., "Automated anatomical labeling of activations in SPM using a macroscopic anatomical parcellation of the MNI MRI single-subject brain," *Neuroimage*, vol. 15, no. 1, pp. 273–289, 2002.
- [29] S. M. Smith et al., "Network modelling methods for FMRI," *Neuroimage*, vol. 54, no. 2, pp. 875–891, 2011.
- [30] X. Chen et al., "High-order resting-state functional connectivity network for MCI classification," *Human Brain Map.*, vol. 37, no. 9, pp. 3282–3296, 2016.
- [31] H. Peng, F. Long, and C. Ding, "Feature selection based on mutual information criteria of max-dependency, max-relevance, and min-redundancy," *IEEE Trans. Pattern Anal. Mach. Intell.*, vol. 27, no. 8, pp. 1226–1238, Aug. 2005.
- [32] K. A. Garrison, D. Scheinost, E. S. Finn, X. Shen, and R. T. Constable, "The (in) stability of functional brain network measures across thresholds," *Neuroimage*, vol. 118, pp. 651–661, Sep. 2015.
- [33] P. Tewarie, E. van Dellen, A. Hillebrand, and C. J. Stam, "The minimum spanning tree: An unbiased method for brain network analysis," *Neuroimage*, vol. 104, pp. 177–188, Jan. 2015.
- [34] S. J. Press and S. Wilson, "Choosing between logistic regression and discriminant analysis," *J. Amer. Stat. Assoc.*, vol. 73, no. 364, pp. 699–705, 1978.
- [35] K. Shah, H. Patel, D. Sanghvi, and M. Shah, "A comparative analysis of logistic regression, random forest and KNN models for the text classification," *Augmented Human Res.*, vol. 5, no. 1, pp. 1–16, 2020.
- [36] A. Fornito, A. Zalesky, and M. Breakspear, "Graph analysis of the human connectome: Promise, progress, and pitfalls," *Neuroimage*, vol. 80, pp. 426–444, Oct. 2013.
- [37] T. Alakörkkö, H. Saarimäki, E. Glerean, J. Saramäki, and O. Korhonen, "Effects of spatial smoothing on functional brain networks," *Eur. J. Neurosci.*, vol. 46, no. 9, pp. 2471–2480, 2017.
- [38] A. M. Triana, E. Glerean, J. Saramäki, and O. Korhonen, "Effects of spatial smoothing on group-level differences in functional brain networks," *Netw. Neurosci.*, vol. 4, no. 3, pp. 556–574, 2020.
- [39] L. Zhang et al., "Deep fusion of brain structure-function in mild cognitive impairment," *Med. Image Anal.*, vol. 72, Aug. 2021, Art. no. 102082.
- [40] S. H. Hojjati, A. Ebrahimzadeh, and A. Babajani-Feremi, "Identification of the early stage of Alzheimer's disease using structural MRI and resting-state fMRI," *Front. Neurol.*, vol. 10, p. 904, Aug. 2019.
- [41] A. Khazaee, A. Ebrahimzadeh, and A. Babajani-Feremi, "Classification of patients with MCI and AD from healthy controls using directed graph measures of resting-state fMRI," *Behav. Brain Res.*, vol. 322, pp. 339–350, Mar. 2017.
- [42] K. Grill-Spector, Z. Kourtzi, and N. Kanwisher, "The lateral occipital complex and its role in object recognition," *Vis. Res.*, vol. 41, nos. 10–11, pp. 1409–1422, 2001.
- [43] A. Schremm, M. Novén, M. Horne, P. Söderström, D. van Westen, and M. Roll, "Cortical thickness of planum temporale and pars opercularis in native language tone processing," *Brain Lang.*, vol. 176, pp. 42–47, Jan. 2018.
- [44] M. S. Koyama, D. O'Connor, Z. Shehzad, and M. P. Milham, "Differential contributions of the middle frontal gyrus functional connectivity to literacy and numeracy," *Sci. Rep.*, vol. 7, no. 1, 2017, Art. no. 17548.
- [45] B. Caplan, J. DeLuca, and J. S. Kreutzer, *Encyclopedia of Clinical Neuropsychology*. Cham, Switzerland: Springer, 2010.
- [46] R. J. Maddock, A. S. Garrett, and M. H. Buonocore, "Remembering familiar people: The posterior cingulate cortex and autobiographical memory retrieval," *Neuroscience*, vol. 104, no. 3, pp. 667–676, 2001.
- [47] Z. Ning, Q. Xiao, Q. Feng, W. Chen, and Y. Zhang, "Relation-induced multi-modal shared representation learning for Alzheimer's disease diagnosis," *IEEE Trans. Med. Imag.*, vol. 40, no. 6, pp. 1632–1645, Jun. 2021.
- [48] X. Zhang, J. Liu, Y. Chen, Y. Jin, J. Cheng, and A. D. N. Initiative, "Brain network construction and analysis for patients with mild cognitive impairment and Alzheimer's disease based on a highly-available nodes approach," *Brain Behav.*, vol. 11, no. 3, 2021, Art. no. e02027.
- [49] G. Zamboni et al., "Resting functional connectivity reveals residual functional activity in Alzheimer's disease," *Biol. Psychiat.*, vol. 74, no. 5, pp. 375–383, Sep. 2013.
- [50] B. Lei et al., "Diagnosis of early Alzheimer's disease based on dynamic high order networks," *Brain Imag. Behav.*, vol. 15, no. 1, pp. 276–287, 2021.



Weiping Wang received the Ph.D. degree in telecommunications physics electronics from Beijing University of Posts and Telecommunications, Beijing, China, in 2015.

She is currently a Professor with the Department of Computer and Communication Engineering, University of Science and Technology Beijing, Beijing. She received the National Natural Science Foundation of China, the Postdoctoral Fund, and the Basic Scientific Research Project. Her current research interests include brain-like computing, complex network, and nonlinear system control.



Shunqi Zhang received the bachelor's degree from the University of Jinan, Shandong, China, in 2020. He is currently pursuing the M.E. degree from the University of Science and Technology Beijing, Beijing, China.

His current research interests is medical image processing of Alzheimer's disease.



Zhen Wang received the Ph.D. degree from Hong Kong Baptist University, Hong Kong, in 2014.

He is a Professor with the School of Artificial Intelligence, Optics and Electronics, Northwestern Polytechnical University, Xi'an, China. His current research interests include complex networks, evolutionary game, and data science.



Xiong Luo received the Ph.D. degree in computer applied technology from Central South University, Changsha, China, in 2004.

He is currently a Professor with the School of Computer and Communication Engineering, University of Science and Technology Beijing, Beijing, China. His current research interests include neural networks, machine learning, and computational intelligence.



Ping Luan received the Ph.D. degree in neurology from Southern Medical University, Guangdong, China, in 2008.

She is an MD and the PI of Medical Center, Shenzhen University, Shenzhen, China, the Chief Physician/Professor, State-Level Leading Talents in Shenzhen, the Director of Alzheimer's Disease Clinical Research Center, Guangdong Second Provincial General Hospital, Shenzhen University, Shenzhen. She has specialized in the basic and clinical research of neurodegenerative diseases.



Alexander Hramov received the Ph.D. degree in physical from Saratov State University, Saratov, Russia, in 1996.

He is the Head of Department in "Automatization, Control and Mechatronics," Saratov State Medical University, Saratov, where he is the Leading Scientist in "Nonlinear Dynamics of Complex Systems with Research and Education Center." He has authored and coauthored of more than 100 papers in scientific journals, several monographs, and is the Head of many scientific projects and grants. His main topics are automatic recognition and analysis of EEG and MEG signals, prevention of epileptic diseases by means of electric stimulation, design of brain-computer interfaces, synchronization in neuronal networks of brain, and modeling of epilepsy.

Dr. Hramov is also a member of national and international societies in his field of expertise.



Jürgen Kurths received the Ph.D. degree in mathematics from University of Rostock, Rostock, Germany, in 1983.

He was a Full Professor with the University of Potsdam, Potsdam, Germany, from 1994 to 2008. Since 2008, he has been a Professor of Nonlinear Dynamics, Humboldt University, Berlin, Germany, and the Chair of the Research Domain Transdisciplinary Concepts, Potsdam Institute for Climate Impact Research, Potsdam, and the Sixth-Century Chair of Aberdeen University, Aberdeen, U.K., since 2009. He has authored over 500 papers that are cited over 18 000 times (H-factor: 57). His primary research interests include synchronization, complex networks, and time series analysis and their applications.

Prof. Kurths received the Alexander von Humboldt Research Award from CSIR, India, in 2005, and an Honorary Doctorate from the Lobachevsky University Nizhny Novgorod in 2008 and one from the State University Saratov in 2012. He is an Editor of journals, such as *PLoS ONE*, the *Philosophical Transactions of the Royal Society A*, the *Journal of Nonlinear Science*, and *Chaos*. He became a member of the Academia Europaea in 2010 and the Macedonian Academy of Sciences and Arts in 2012. He is a Fellow of the American Physical Society.

He is currently a Professor with the University of Potsdam, Potsdam, Germany, from 1994 to 2008. Since 2008, he has been a Professor of Nonlinear Dynamics, Humboldt University, Berlin, Germany, and the Chair of the Research Domain Transdisciplinary Concepts, Potsdam Institute for Climate Impact Research, Potsdam, and the Sixth-Century Chair of Aberdeen University, Aberdeen, U.K., since 2009. He has authored over 500 papers that are cited over 18 000 times (H-factor: 57). His primary research interests include synchronization, complex networks, and time series analysis and their applications.

Prof. Kurths received the Alexander von Humboldt Research Award from CSIR, India, in 2005, and an Honorary Doctorate from the Lobachevsky University Nizhny Novgorod in 2008 and one from the State University Saratov in 2012. He is an Editor of journals, such as *PLoS ONE*, the *Philosophical Transactions of the Royal Society A*, the *Journal of Nonlinear Science*, and *Chaos*. He became a member of the Academia Europaea in 2010 and the Macedonian Academy of Sciences and Arts in 2012. He is a Fellow of the American Physical Society.



Chang He received the bachelor's degree from Tianjin University of Science and Technology, Tianjin, China, in 2020. She is currently pursuing the M.E. degree with the University of Science and Technology Beijing, Beijing, China.

Her current research interests is computational modeling of Alzheimer's disease.



Jianwu Li received the Ph.D. degree in telecommunications physics electronics from Beijing University of Posts and Telecommunications, Beijing, China, in 2015.

He is currently the Deputy Director of Sensor Intelligence Technology Center of Frontier Technology Research Institute, Beijing Institute of Technology, Beijing, and a Professor with the Department of Engineering, Huanghe Science and Technology College, Zhengzhou, China. His research focuses on cutting-edge electronic information technologies and industrial applications, such as Internet of Things, industrial Internet, and sensing and edge computing.